A BLADE-ON-PETIOLE ortholog regulates floral proximodistal patterning in *Torenia fournieri*

Shihao SU (sushh7@mail.sysu.edu.cn)
Sun Yat-sen University
Yawen Lei
Sun Yat-sen University
Xuan Zhou
Sun Yat-sen University
Takamasa Suzuki
Chubu University https://orcid.org/0000-0002-1977-0510
Wei Xiao
Sun Yat-sen University
Tetsuya Higashiyama
Institute of Transformative Biomolecules

Article

Keywords: floral organ, proximodistal axis, BOP, ALOG, corolla differentiation, Torenia fournieri

Posted Date: August 2nd, 2022

DOI: https://doi.org/10.21203/rs.3.rs-1879205/v1

Version of Record: A version of this preprint was published at Nature Communications on August 8th, 2023. See the published version at https://doi.org/10.1038/s41467-023-40399-3.

Abstract

The three-dimensional shape of a flower is integrated by morphogenesis along different independent floral axes. Differentiation along the floral proximodistal axis is tightly linked to specification of pollinators; however, it is still obscure how a flower patterns its proximodistal axis. The corolla of a *Torenia fournieri* flower exhibits strong differentiation along the proximodistal axis, including a distal petal lobe region, an intermediate corolla tube, and a proximal corolla neck region that is control by an ALOG (*Arabidopsis* LSH1 and *Oryza* G1) family homolog, TfALOG3. In this study, we report a floral specific *BOP* (*BLADE-ON-PETIOLE*) gene, *TfBOP2*, which is predominantly expressed in the proximal region of corolla. CRISPR knockout mutants of *TfBOP2* have shorter proximal corolla tube and longer distal lobe region, with ectopic growth of conical cells in the fusion boundaries of corolla tube, consistent with its expression pattern as a proximal regulator. Mutants of BOP homologs in *Arabidopsis thaliana* also shows developmental defects in petal proximal region, favoring a conserved role of BOPs among different species. Genetic analysis demonstrates interaction between *TfBOP2* and *TfALOG3* in the control of corolla proximodistal patterning, since double mutants have shortest proximal corolla tube, while exhibiting normal boundary fusion. We further find that TfALOG3 physically interacts with TfBOP2, and can recruit TfBOP2 to the nucleus region, indicating their function possibly as a dimer. Our study unveils a plant universal BOP-ALOG complex being recruited to regulate flower proximodistal patterning of *T. fournieri*.

Introduction

Floral organs are hypothesized to be evolved from the ground state of leaf-like organs (1). The final floral shape of angiosperm varies considerably, and this morphological diversity can be achieved via multiple ways, including changing floral symmetry, altering organ number or size, elaborating individual organ, and making organ fusion (2, 3). The specific shape of a flower is a product from long history of plant-pollinator interactions (4). For example, the formation of corolla tube (fusion of petals) in most asterids lineages has been regarded as a morphological innovation, which possibly driven by animal pollinators and basically distinguishing asterids from rosids (5).

The three-dimensional shape of a flower is integrated through differentiation in an organized fashion along different floral axes, such as the radial, dorsoventral and proximodistal axes. Floral radial and dorsoventral axes are established *de novo* within the plane of floral meristem: radial axis defines four concentric whorls of floral organs (i.e. sepal, petal, stamen and carpel) from the outermost to the central part of a floral meristem; while the dorsoventral axis describes the relationship of different organs within one whorl (namely, dorsal, lateral and ventral). Several ancient modular programs have been discovered to explain the conserved developmental organogenesis of flowers along these two axes in various species (2, 6). According to the ABC model, the identities of four concentric floral organs along the radial axis are controlled by three classes of homeotic genes: A genes are required for the identities of sepals and petals, B genes are essential for petals and stamens, while C genes confer the identities of stamens and carpels (7). Variations in organ identity are generally the results of changes in these organ identity

genes, such as petaloid bract of *Cornus florida*, or the specification of lip in orchid flowers (8–10). Differentiation along the dorsoventral axis results from combinatory roles of TCP and MYB transcription factors: specifically, CYCLOIDEA-like (CYC-like) TCP protein and RADIALIS-like (RAD-like) MYB protein play together as dorsal factors; while another DIVARICATA-like (DIV-like) MYB protein provides a ventralising signal (2, 11–13).

The floral proximodistal axis is defined by polarized growth of floral organ primordia, which initiate away from the plane of floral meristem, and are elaborated by different cell and tissue types (14). In terms of petal, a billboard organ of an entomophilous flower to attract its pollinators, differentiation along the proximodistal axis is evident in pigmentation pattern, epidermal micromorphology or specification of the petal surface, and such differentiation becomes a major component of floral diversity in nature. In Arabidopsis, *JAGGED* (*JAG*) encodes a zinc finger transcription factor, promoting distal growth of leaf and petal as *jag* mutant processes serrated distal organ margins (15, 16). The *cin* (*cincinnata*) mutant from *Antirrhinum majus* has larger leaves due to excess growth of leaf margin and smaller petal lobes that are correlating with specific expression of *CIN* in distal corolla lobes, favoring its roles in regulating growth and differentiation of both leaf and petal (17). In spite of these findings, factors specifically involved in the floral proximodistal patterning have yet to be identified.

The genetic regulation of plant proximodistal patterning is mainly studied using leaf as a model. *Class I KNOTTED* homeobox (*KNOX I*) genes, which promote indeterminate growth, are expressed in the meristematic tissues (14). Mutant analyses indicate that ectopic expression of *KNOX I* genes in leaf results in changes of leaf proximodistal patterning, as the cases in the gain-of-function maize mutants (18). A typical leaf of eudicots can be subdivided into two regions, including a proximal petiole and a distal blade. In Arabidopsis, *bop1* (*blade on petiole1*) and *bop2* (*blade on petiole2*) mutants have ectopic lobed blades along the petiole, suggesting that BOP transcription factors suppress blade outgrowth and are indispensable for the proximodistal patterning of a leaf (19–21). In legume species including pea and *Lotus japonicus*, *BOP* genes are involved in the differentiation of stipules, leaflet-like organs in the proximal part of leaves (22, 23). In monocots, such as rice and barley, the proximal region of a leaf is called as sheath. The monocots *BOP* genes show strong expressions in leaf primordia as well as the proximal sheath margins, and mutant analyses indicate that they are essential for proper sheath-blade ratio by promoting sheath differentiation and suppressing blade development (24, 25). Furthermore, BOP proteins are also involved in many other biological processes, including organ boundary formation, plant architecture establishment, nodule development and abscission zone formation (26). However, whether BOPs are involved in floral proximodistal patterning, and if they have a role in the formation of corolla tube, are still mysterious.

To investigate the molecular mechanisms involved in floral proximodistal patterning, we studied a Linderniaceae species, *Torenia fournieri*, whose corolla can be divided into several sub-regions due to different pigmentations along its proximodistal axis. The distal part of petals forms a lobe region, in which separated lateral and ventral petal lobes have violet pigmented spots; a middle corolla region forms a conical tube, which itself can be further subdivided into a distal part with light purple pigments

and a proximal part with abundant yellow carotenoids; and a corolla base which specified into an inflated neck region, which may help flowers to prevent raindrops from contacting the nectar inside corolla. We recently reported that *TfALOG3*, an *ALOG* (*Arabidopsis LSH1* and *Oryza G1*) family gene, is expressed in the epidermal cells of proximal corolla neck, and the *TfALOG3* loss-of-function mutants fail to differentiate into such organ (27). Since ALOG proteins in tomato and pea have shown to interact with BOP proteins, we propose the existence of a conserved protein dimer formed by BOP and ALOG within plants (28–30). Here, we isolated a floral specific BOP protein from *T. fournieri*, *TfBOP2*, which is predominantly expressed in the proximal corolla regions. Loss-of-function mutants of *TfBOP2* show developmental defects in proximal corolla differentiation, and this is correlated to its expression pattern. The functions of BOP proteins in floral proximodistal patterning are evolutionarily conserved cross eudicots. We also found genetic and physical interactions between TfALOG3 and TfBOP2, favoring our hypothesis that a conserved BOP-ALOG module has been recruited to regulate flower proximodistal patterning of *T. fournieri*.

Results

TfBOP2 expresses predominantly in the proximal regions of corolla

We isolated two *BOP* genes from the genome of *T. fournieri*. Sequence alignments using TfBOP1/2 and Arabidopsis BOP1/2 proteins suggest three conserved domains in these proteins (Fig. S1), including a BTB/POZ domain in the N-terminus, an ANK-repeat domain in the C-terminus, and an unknown domain DUF3420 that is partially overlapped with the ANK-repeat domain. To understand the evolutionary history of *BOP*-like genes, we carried out phylogenetic analysis by using *BOP*-like genes from different plant lineages. The phylogenetic tree indicates that *BOP*-like genes originate anciently and distribute in various species (Fig. 1A). Multiple times of duplication events of *BOP*-like genes occurred independently in different plant lineages including the moss (*Physcomitrella patens* (*Pp*)), monocots (*Spirodela polyrhiza* (*Sp*), *Ananas comosus* (*Ac*), *Zostera marina* (*Zma*), *Oryza sativa* (*Os*), *Zea mays* (*Zm*)) and dicots (*Solanum lycopersicum* (*Sl*) , *Medicago truncutula* (*Mt*), *Malus domestica* (*Md*), *Populus trichocarpa* (*Pt*), *Manihot esculenta* (*Me*), *Arabidopsis thaliana* (*At*), *Boechera stricta* (*Bs*), *Capsella grandiflora* (*Cg*), *Sesamum indicum* (*Si*), *Antirrhinum majus* (*Am*), *Lindernia brevidens* (*Lb*), *Lindernia subracemosa* (*Ls*) and *Torenia fournieri* (*Tf*)). *Torenia* belongs to the family of Linderniaceae, which contains two specific sub-clades of *BOP* genes (Fig. 1A), signifying a duplication event occurred prior to the divergence of *Torenia* and *Lindernia* genus. We further want to know whether the two paralogs of *Torenia* BOP function divergently or equally.

We examined the expression patterns of two *TfBOP*s using reverse transcription (RT)-PCR and RNA *in situ* hybridization assays. RT-PCR shows that *TfBOP1* is expressed in various tissues, with high expression in roots, vegetative and reproductive apexes; however, *TfBOP2* is specifically expressed in the floral buds, suggesting functional diversification of these two paralogs (Fig. 1B). RNA *in situ* hybridization assays

demonstrate that *TfBOP1* is strongly expressed in the early stages of floral meristems, whereas *TfBOP2* is not (Fig. 1C-D). In stage 6 (Fig. 1E-F) and stage 8 (Fig. 1G-H), both genes are highly expressed in the stamens and ovules; however, they show divergent expression patterns in the corolla. Compared with the controls using sense probes (Fig. S2), signals using antisense probes of *TfBOP1* are dispersed in the whole corolla, while *TfBOP2* antisense probes show strong signals in the proximal region of corolla. This specific expression of *TfBOP2* gives strong evidence of its role in corolla proximodistal patterning.

TfBOP2 is indispensable to corolla proximodistal patterning

We then explored the function of TfBOP2 by obtaining the *TfBOP2* loss-of-function mutants. A CRISPR/Cas9 plasmid containing three *TfBOP2*-specific guide RNAs was constructed and transformed into *T. fournieri*, and the *TfBOP2* genes from two independent transgenic lines were sequenced prior to further analysis (Fig. S3). We detected different numbers of nucleotides deletions or insertions in the targeted sites of *TfBOP2* genes, leading to frame shift and premature termination (Fig. S3).

We later compared the floral morphologies of the wild type (WT) and the *TfBOP2*-Cas9 plants (Fig. 2). In two *TfBOP2*-Cas9 lines, developmental defects of the proximal corolla region were detected, including the proximal tube and corolla neck (Fig. 2A-C). In the WT, yellow pigments are preferentially accumulated in the proximal region of corolla tube; however, these pigments become lighter and ectopically shift to corolla bottoms of *TfBOP2*-Cas9 plants (Fig. 2A-C). Second, *TfBOP2*-Cas9 flowers often show abnormities in corolla tube fusion. Compared with the WT, flowers of *TfBOP2*-Cas9 have narrowed corolla tube, leading to distorted corolla forms from the front view (Fig. 2A-C). Moreover, cells in the corolla fusion boundaries become excessively proliferative, as we found ectopic tissues developed on these regions (Fig. 2B-C).

Since epidermal cell morphologies vary along the proximodistal axis, we then compared the corolla epidermis using a scanning electron microscopy. In the WT plant, we divided corolla into five subregions along the proximodistal axis, including one lobe region (Lobe) and four types of tube regions (Tube-1-Tube-4) (Fig. 2D). Conical cells, flat conical cells, puzzle-shaped cells with wavy edges, puzzle-shaped cells with smooth edges and rectangular cells are the representative cell types of five regions, respectively (Fig. 2D). In addition, trichomes are found specifically in the distal Tube-1 region of WT's corollas (Fig. 2D). Compared with WT, only the epidermal cells from corolla proximal regions are affected in *tfbop2* mutant (Fig. 2D). Trichomes are ectopically found in all regions of mutant's corollas, including Tube-3 and -4 regions; Second, epidermal cells of the Tube-2 region are shorter, while those of the Tube-3 region are puzzle-shaped cells with wavy edges, like WT's Tube-2 region; In addition, epidermal cells of the

Tube-4 region become smaller compared with the WT's (Fig. 2D). These results demonstrate a specific role of TfBOP2 in the control of proximal corolla differentiation.

TfBOP2 controls corolla lobe-tube ratio by inhibiting lobe outgrowth

To understand the developmental defects of *TfBOP2*-Cas9 flowers, we compared floral organogenesis of WT and *tfbop2* under a scanning electron microscopy (Fig. 3). In stage 6, stamens are larger than petals. General floral morphologies of WT and *tfbop2* seem similar, however, the relative length ratios of corolla lobe versus tube is increased in the mutant (2.03 of WT and 4.71 of *tfbop2*). Increased lobe-tube ratios are also found in later stages (stage 7, 1.37 of WT and 0.92 of *tfbop2*; stage 13, 0.56 of WT and 0.93 of *tfbop2*), suggesting TfBOP2's function as a suppressor in lobe outgrowth.

As mentioned before, TfBOP2-Cas9 flowers also exhibit developmental abnormities in corolla tube formation. We observed these defects starting from stage 7 (Fig. 3C-D). We found enlarged tissues formed in the fusion margins of mutants' corolla tube, and these tissues further proliferate along with the development of flowers (Fig. 3E-I). We also noticed that epidermal cells on these ectopic tissues are small and spherical, which are morphologically similar with epidermal cells in distal lobe regions (Fig. 3J-K, 2D). These findings favor a hypothesis that loss of TfBOP2 results in distalization of proximal corolla.

TfBOP2 regulates corolla differentiation possibly through targeting genes related to meristem and boundary formation

To investigate how TfBOP2 is involved in corolla differentiation, we carried out transcriptome sequencing using total RNA from stage 10 corollas. We further performed differential gene expression between WT and *tfbop2* using edgeR (Tab. S1). There are 1842 significantly up-regulated and 3174 down-regulated contigs in *tfbop2* mutant (FDR<0.001). Gene Ontology (GO) enrichment was performed using the contigs that are significantly changed in *tfbop2* mutant (Tab. S2). Among the significantly enriched GO terms (P<0.05), terms annotated as protein complex assembly, auxin polar transport, pigment biosynthesis, cell wall metabolism, regulation of anatomical structure and developmental cell growth are included (Fig. 4A). The differentially expressed genes (DEGs) contain many candidates acting as potential downstream targets of TfBOP2, including factors involved in meristem and boundary formation, epidermis differentiation, carotenoid biosynthesis, cell wall modification, and auxin signaling (Fig. 4B, Tab. S2). These GO terms and DEGs are correlated with the morphological changes in *tfbop2* flowers. Among the 7 DEGs related to meristem and boundary formation, two *KNOX I* genes (*TfB098546* and *TfB076160*) are contained, with significant up-regulation in *tfbop2* mutant (Fig. 4B). *TfB098546* and *TfB076160* are the orthologs of Arabidopsis KNAT2/6 (Fig. S4), and TfBOP2 may be able to restrict their expressions at the flower base, thus coordinating corolla tube fusion along the proximodistal axis.

BOPs' function in patterning floral proximodistal axis is conserved in Arabidopsis

To understand whether function of BOPs in patterning floral proximodistal axis is conserved or not, we examined the flower morphologies of WT and *bop1 bop2* mutant of Arabidopsis (Fig. 5). Although possessing a choripetalous corolla, cell differentiation also manifests along the proximodistal axis, as a WT Arabidopsis petal has a white distal blade and a greenish proximal claw (Fig. 5A). In *bop1 bop2* mutant, however, the white blade regions become longer while the proximal claws are sharper (Fig. 5B). We further compared the petal epidermis of these flowers. Epidermal cells are generally similar in different regions, we found ectopic conical cells in the R2 region of *bop1 bop2* mutant, suggesting an elongated blade region (Fig. 5C-D, Fig. S5). Together with our findings in *T. fournieri*, we proposed that BOPs' function in patterning floral proximodistal axis is conserved during plant evolution.

TfBOP2 genetically interacts with *TfALOG3* controlling proximodistal patterning of corolla

We previous reported that flowers of *TfALOG3*-Cas9 show specific loss of proximal corolla necks (Fig. 6A), and water can enter to the bottom of corolla and thus dilute the nectar (27). This phenomenon was also observed when we applied water into flowers of *TfBOP2*-Cas9 plants (Fig. S6). In the WT, a clear boundary is observed in the constriction region with hairs that connects proximal yellow tube and corolla neck; however, it becomes no longer apparent in *TfALOG3*-Cas9 or *TfBOP2*-Cas9 flowers (Fig. S6). *TfBOP2* and *TfALOG3* loss-of-function mutants share similar developmental defects within the proximal corolla, favoring genetic interaction between these genes; hence, we investigated morphology of double mutants. Similar to *tfbop2*, double mutant of *TfALOG3* and *TfBOP2* (*tfalog3-40 tfbop2-2*) also processes a distorted corolla (Fig. 2B, 6A). Interestedly, unlike *tfbop2*, defect in corolla fusion is largely rescued, as we could not found ectopically developed tissues at the fusion margins (Fig. 6A). In addition, we noticed that the carotenoids enriched tube region in *tfalog3-40 tfbop2-2* is strikingly shortened compared with either *tfalog3* or *tfbop2* (Fig. 6B-D). We further measured lengths of different corolla regions among four genotypes (Fig. 6C-D). In *tfalog3*, only proximal tube region is shorter than the WT's; while *tfbop2* has a longer distal lobe with a shorter tube; in the double mutant, distal lobe is longer as *tfbop2* whereas possessing a shortest proximal tube.

As corolla proximodistal patterning is also evident in epidermal cell morphology, we also examined the corolla epidermal cells in single and double mutants (Fig. 6E). Typical five types of epidermal cells are also found in *tfalog3-40*, and compared with WT, only rectangular cells in Tube 4 region become smaller, consistent with our previous findings. In *tfalog3-40 tfbop2-2,* however, epidermal cells in T2, T3 and T4 regions are changed, and we ectopic trichomes in the T3 and T4 regions of its corolla tube as the case in *tfbop2* (Fig. 6D). Altogether, these results favor genetic interaction between *TfALOG3* and *TfBOP2*.

TfBOP2 physically interacts with TfALOG3

We further examined the subcellular localizations of TfALOG3 and TfBOP2 by transient expression of fused proteins in tobacco leaf epidermal cells (Fig. 7A). We found that TfALOG3-Venus proteins are located in the nucleus, and this is consistent with our previous data using Arabidopsis mesophyll protoplasts (31). Unlike TfALOG3-Venus, transiently expressed TfBOP2-mRuby2 proteins show both cytoplasmic and nuclear localization (Fig. 7A). We next want to know if the localization of TfBOP2 proteins can be affected by co-expression of TfALOG3. The result shows that TfBOP2-mRuby2 signals exclusively shifted to the nuclear region when *TfALOG3* was co-transformed, suggesting that TfBOP2 can be recruited to nucleus by TfALOG3 possibly through forming a transcriptional complex (Fig. 7B).

To verify this hypothesis, we performed bimolecular fluorescence complementation (BiFC) and yeast two hybrid (Y2H) assays (Fig. 7C-D). BiFC assays confirm that TfBOP2 interacts with TfALOG3 in the nucleus (Fig. 7C). We also demonstrated that full length of TfBOP2 proteins interact with TfALOG3 in yeast (Fig. 7D). Since there are three major domains on TfBOP2, to understand how TfBOP2 interacts with TfALOG3, we further split TfBOP2 into different parts and performed Y2H assays (Fig. S7). Full length of TfBOP2 shows the strongest interaction and its DUF3420, ANK-repeat and C-terminal domains manifest a weaker interaction (Fig. S7). These findings provide biochemical evidences to the formation of BOP-ALOG complex and favor a conserved working module of BOP and ALOG factors in various plant lineages.

Discussion

The formation of corolla tube has evolved multiple times independently and is considered as a developmental innovation of asterids, which contain many species with morphologically complex floral structures (32). Diversification in corolla tube helps asterids species to attract different groups of animal pollinators, which in turn, promotes rapid plant speciation (33). The corolla of *T. fournieri* displays a typical bee pollination syndrome along the proximodistal axis (Fig. 2), with a distal lobe region functioning as a billboard and landing platform, an intermediate tube with contrasting carotenoid pigments as nectar guide, and a proximal neck region which helps to protect the nectar. Such proximodistal differentiation, evident in various flowers, is an outstanding example of plant evolution and reproductive success, raising questions about its origin from the perspective of molecular genetics.

In *Torenia*, two paralogs of *BOP* genes exhibit distinct expression patterns indicating functional divergence after duplication (Fig. 1). *TfBOP1* is expressed in various tissues including vegetative and floral meristems, and such pleotropic expression pattern is similar to most previous reported *BOP* genes of dicots and monocots, suggesting an ancestral function of *BOP*s. *TfBOP2* displays predominant expression in floral tissues, similar to the tobacco *BOP* gene *NtBOP2*. *NtBOP2* is primarily expressed at the base of corolla called abscission zone, and alteration in its expression brings defects not in the

course of corolla growth and development but in corolla abscission (34). We detected specific expression of *TfBOP2* from stage 6, rather than early stages like floral meristem or petal primordia, suggesting its functions after petal initiation (Fig. 1). Consistent with its expression pattern, we observed obvious developmental defects from stage 6 of *tfbop2* flowers (Fig. 3). The proximal corolla regions of *tfbop2*, including proximal part of corolla tube and proximal corolla neck, become abnormal, and this is also evident in epidermal cell pattern and pigmentation (Fig. 2, 6). During the floral ontogeny of *T. fournieri*, five petal primordia emerge independently and later fuse together at their bases after stage 6, supporting a characteristic of late sympetaly (11). We also observed abnormal petal fusion in mutant flowers, favoring a hypothesis that *TfBOP2* simultaneously coordinates proximal corolla differentiation and sympetaly. In spite of these findings, however, we should notice that other proximal factors are yet to be unveiled due to the following two reasons: First, the proximal identity of *tfbop2* corolla is not completely lost, and we can still observe proximodistal differentiation in *tfbop2* flowers; Second, organ proximodistal polarity is thought to be established as early as the initiation of petal primordia, thus other proximal factors can be recruited in earlier developmental stages.

We investigated possible downstream targets of TfBOP2 through transcriptome sequencing. Genes involved in meristem and boundary formation, epidermis differentiation, carotenoid biosynthesis, cell wall modification, and auxin signaling are significantly changed in mutant (Fig. 4). Among these genes, we noticed that two *KNOX I* genes, *TfKNAT2* and *TfKNAT6*, are significantly up-regulated in *tfbop2* mutant (Fig. 4B). There are five KNOX I proteins in *T. fournieri*, and TfKNAT2 and TfKNAT6 are orthologous proteins of Arabidopsis KNAT2 and KNAT6 (Fig. S4). In Arabidopsis *bop1-1* mutant, three *KNOX I* genes, *KNAT1*, *KNAT2* and *KNAT6*, are expressed in an expanded region of leaf, suggesting that BOP negatively regulates *KNOX I* genes and thus changes the meristematic activity of leaf cells (21). The repression of *KNOX I* genes at the leaf base may generated through direct activation of *ASYMMETRIC LEAVES2* (*AS2*), which promotes adaxial leaf polarity and inhibits the expression of *KNOX I* genes possibly by the formation of protein dimer with ASYMMETRIC LEAVES1 (AS1) (21). Interestingly, Arabidopsis BOPs are likely regulate *KNOX I* differentially in inflorescence, as *KNAT6* is misexpressed in the *BOP1* gain-of-function plants and, such misexpression is required for its inflorescence defects (38). *TfKNAT2* and *TfKNAT6* are upregulated in *TfBOP2* loss-of-function mutants, suggesting that TfBOP2 can negatively regulate *KNOX I* activities in *Torenia*. Numerous work demonstrates that KNOX I proteins function in pluripotent cells of meristems as well as differentiating cells of various organs, and are vital for primordium initiation, boundary formation and meristem maintenance (35). Hence, we infer that defects of corolla fusion in *tfbop2* flowers rely on the ectopic expressions of *TfKNAT2* and *TfKNAT6*.

In this study, we found that TfBOP2 works together with TfALOG3 in the control of floral proximodistal patterning. Either *TfALOG3* or *TfBOP2* is highly expressed in the proximal region of corollas (Fig. 1), suggesting that they may function together as a module regulating corolla patterning (27). Although similar defects of proximal corolla have been observed, their developmental defects are not identical. First, unlike *tfalog3*, the distal lobe regions are longer and the whole tubes of *tfbop2* mutant are affected, suggesting that TfBOP2 functions in a broader region than TfALOG3 (Fig. 6). Second, in *tfalog3*, proximal corolla neck is completely lost (27), however, in *tfbop2*, we can still figure out a constriction region at the

base, although such structure is no longer as same as the WT's (Fig. 6, S6). This is reasonable since the expression of TfALOG3, which is responsible for the formation of constriction, has not been changed in *tfbop2* mutant. When TfALOG3 is further mutated, the constriction region together with the connected base is expected to be lost, and this is evident in a shortened yellow tube of *tfalog3 tfbop2* double mutant (Fig. 6). Interestingly, corolla fusion defects in *tfbop2* mutant have been largely rescued in the double mutants, indicating that TfALOG3 may antagonizes TfBOP2 activity in the corolla boundary formation (Fig. 6). These data favor that TfBOP2 and TfALOG3 have overlapped roles controlling flower proximodistal patterning.

We further demonstrated that TfBOP2 can physically interact with TfALOG3, and with the presence of TfALOG3, TfBOP2 proteins are recruited to nucleus (Fig. 7A-B). In fact, BOP-like and ALOG-like proteins show similar ability to form protein complexes in other plant lineages. In tomato, three *BOP* genes are redundantly expressed in the vegetative and transition meristem, and by forming different complexes, they act synergistically with TMF, an ALOG family protein, and thus regulate inflorescence architecture and leaf axil patterning (28, 29). *COCHLEATA* (*COCH*), a *BOP1/2* ortholog from *Pisum sativum*, is expressed in various tissues, which has pleotropic roles in multiple developmental processes including nodule development and lateral organ morphogenesis (30). COCH shows interaction with an ALOG protein, SYMMETRIC PETALS 1 (SYP1), and plays a role in petal asymmetry and nodule development (30). These studies indicate the general existence of BOP-ALOG protein complexes, at least among eudicots.

To summarize, we report a floral specific BOP from *T. fournieri*, TfBOP2, which acts synergically with TfALOG3 and couples both proximal corolla development and sympetaly. In the future, it is of interests to study how BOP-ALOG complexes work in various biological processes, and to unveil the nature of floral proximodistal patterning.

Materials And Methods

Plant materials and transformation

Plants of *T. fournieri*, *A. thaliana*, *Nicotiana benthamiana* were maintained at 25°C under a 16 h light: 8h dark cycle. To carry out plant transformation, leaf disks of *T. fournieri* were collected from the sterile plants grown on 1/2 MS culture medium. The CRISPR/Cas9 binary vector was produced according to the published protocol (39). Transformation of the CRISPR/Cas9 binary vector into WT plants was performed as previously reported (11, 27, 40).

Phylogenetic and expression analysis

To figure out the phylogenetic relationship of *BOP* genes in plants, we collected homologous gene sequences from Phytozome (https://phytozome.jgi.doe.gov) and other published genome database. Alignments of nucleotide sequences were performed in MEGA X (41). The Maximum-likelihood tree of *BOP* genes under 500 replicates of bootstrap iterations was also generated by MEGA X. For RT-PCR

analysis, total RNA and the cDNA templates were prepared as reported (27). *β-Actin* (*TfACT3*) expression was used as an internal control. For RNA *in situ* hybridization, inflorescences were fixed in FAA fixative (10% formalin solution, 5% acetic acid and 50% ethanol). The tissues were then embedded with Paraplast-plus (Sigma-Aldrich) after treatment with multiple ethanol and xylene solutions. The sense and antisense probes were labeled with digoxigenin-UTP. Hybridization processes were performed as described (42). All the primers used in this study were listed in Table S4.

Protein localization and interaction

To generate the constructs for subcellular localization, Venus protein was fused to the C terminus of TfALOG3 and mRuby2 was fused to the C terminus of TfBOP2, respectively. Fused proteins were driven by the CaMV35S promoter. To produce vectors for the BiFC assay, coding sequences of TfALOG3 and TfBOP2 were ligated into split YFP vectors driven by the CaMV35S promoter. The constructed plasmids were transformed into *Agrobacterium tumefaciens* EHA105, and then transfected into tobacco leaves through infiltration. Signals of tobacco leaves were checked after two days using a confocal laser scanning microscopy Zeiss7 DUO NLO. All the primers used here were listed in Table S4.

Microscopy

To compare floral development of different plants, floral buds of different stages were collected and dissected using fine tweezers under a stereomicroscope. To observe corolla epidermal cells, mature corollas from various genotypes were cut by a razor blade. Floral buds and corollas were rapidly covered by different types of impression materials to produce the epoxy replica as previously reported (43). The replicas were then observed under a Keyence VHX-D510 microscope.

Transcriptomic analysis

Stage 11 corollas were collected from the WT and *TfBOP2*-Cas9 2# plants. Total RNA was extracted using the RNAqueous-Micro kit and Plant RNA Isolation Aid according to the manual (Ambion). The cDNA libraries were constructed using the TruSeq RNA Sample Preparation kit (Illumina). Sequencing, assembly and annotation of contigs were carried out as previously reported (44). Expression analysis was performed through the EdgeR package using the mapped reads and gene ontology annotations were annotated by the Blast2GO program.

Declarations

Acknowledgement

This work was supported by Guangdong Basic and Applied Basic Research Foundation (No. 2021A1515111139) and the Japan Society for the Promotion of Science (No. 19F19091) and S.S. was supported by an overseas postdoctoral fellowship from Japan Society for the Promotion of Science.

Author contributions

S.S. and T.H. conceived and designed the experiments. S.S. and Y.L. performed most of the experiments; T.S. carried out RNA sequencing and W.X. performed the phylogenetic and RT-PCR analysis. S.S. wrote the manuscript with contributions from all of the authors.

References

1. Sablowski R (2015) Control of patterning, growth, and differentiation by floral organ identity genes. J Exp Bot 4SI(66): 1065–1073.
2. Moyroud E,Glover BJ (2017) The evolution of diverse floral morphologies. Curr Biol 17(27): R941-R951.
3. Fernández-Mazuecos M,Glover BJ (2017) The evo-devo of plant speciation. Nat Ecol Evol 4(1).
4. Darwin CR (1859) *On The Origins of Species by Means of Natural Selection* (London: Murray).
5. Chanderbali AS, *et al.* (2017) Evolution of floral diversity: genomics, genes and gamma. *Philos Trans R Soc Lond B Biol Sci* 1713(372).
6. Shan H, *et al.* (2019) Developmental mechanisms involved in the diversification of flowers. Nat Plants 9(5): 917–923.
7. Coen ES,Meyerowitz EM (1991) The war of the whorls: genetic interactions controlling flower development. Nature 6339(353): 31–37.
8. Su S, *et al.* (2018) An AGAMOUS-like factor is associated with the origin of two domesticated varieties in Cymbidium sinense (Orchidaceae). *Hortic Res-England* 1(5).
9. Su S, *et al.* (2018) Transcriptome-Wide Analysis Reveals the Origin of Peloria in Chinese Cymbidium (Cymbidium sinense). Plant Cell Physiol 10(59): 2064–2074.
10. Feng C, *et al.* (2012) Evolution of bract development and B-class MADS box gene expression in petaloid bracts of Cornus s. l. (Cornaceae). New Phytol 2 196.: 631–643.
11. Su S, *et al.* (2017) The CYCLOIDEA–RADIALIS module regulates petal shape and pigmentation, leading to bilateral corolla symmetry in Torenia fournieri (Linderniaceae). New Phytol 4(215): 1582–1593.
12. Luo D, *et al.* (1996) Origin of floral asymmetry in Antirrhinum. Nature 6603(383): 794–799.
13. Da L, *et al.* (1999) Control of organ asymmetry in flowers of Antirrhinum. Cell 4(99): 367–376.
14. Satterlee JW,Scanlon MJ (2019) Coordination of leaf development across developmental axes. Plants 10(8): 433.
15. Sauret-Gueto S, *et al.* (2013) JAGGED controls Arabidopsis petal growth and shape by interacting with a divergent polarity field. Plos Biol 4(11): e1001550.
16. Ohno CK, *et al.* (2004) The Arabidopsis JAGGED gene encodes a zinc finger protein that promotes leaf tissue development. Development 5(131): 1111–1122.

17. Crawford B, *et al.* (2004) CINCINNATA controls both cell differentiation and growth in petal lobes and leaves of antirrhinum. Plant Physiol 1(135): 244–253.
18. Ramirez J, *et al.* (2009) Distal Expression of knotted1 in Maize Leaves Leads to Reestablishment of Proximal/Distal Patterning and Leaf Dissection. Plant Physiol 4(151): 1878–1888.
19. Hepworth SR, *et al.* (2005) BLADE-ON-PETIOLE–dependent signaling controls leaf and floral patterning in Arabidopsis. The Plant Cell 5(17): 1434–1448.
20. Norberg M, *et al.* (2005) The BLADE ON PETIOLE genes act redundantly to control the growth and development of lateral organs. Development 9(132): 2203–2213.
21. Ha CM (2003) The BLADE-ON-PETIOLE 1 gene controls leaf pattern formation through the modulation of meristematic activity in Arabidopsis. Development 1(130): 161–172.
22. Couzigou J, *et al.* (2012) NODULE ROOT and COCHLEATA maintain nodule development and are legume orthologs of Arabidopsis BLADE-ON-PETIOLE genes. The Plant Cell 11(24): 4498–4510.
23. Magne K, *et al.* (2018) Lotus japonicus NOOT-BOP-COCH-LIKE1 is essential for nodule, nectary, leaf and flower development. Plant J 5(94): 880–894.
24. Toriba T, *et al.* (2019) BLADE-ON-PETIOLE genes temporally and developmentally regulate the sheath to blade ratio of rice leaves. Nat Commun 1(10).
25. Tavakol E, *et al.* (2015) The barley Uniculme4 gene encodes a BLADE-ON-PETIOLE-like protein that controls tillering and leaf patterning. Plant Physiol 1 168.: 164–174.
26. Khan M, *et al.* (2014) BLADE-ON-PETIOLE genes: Setting boundaries in development and defense. Plant Sci 215–216): 157–171.
27. Xiao W, *et al.* (2019) A homolog of the ALOG family controls corolla tube differentiation inTorenia fournieri. Development 16(146): v177410.
28. Xu C, *et al.* (2016) Control of inflorescence architecture in tomato by BTB/POZ transcriptional regulators. Gene Dev 18(30): 2048–2061.
29. Izhaki A, *et al.* (2018) The tomato BLADE ON PETIOLE and TERMINATING FLOWER regulate leaf axil patterning along the proximal-distal axes. Front Plant Sci 9).
30. He L, *et al.* (2020) SYMMETRIC PETALS 1 Encodes an ALOG Domain Protein that Controls Floral Organ Internal Asymmetry in Pea (Pisum sativum L.). International Journal of Molecular Sciences 21(4060.
31. Xiao W, *et al.* (2018) Evolution of ALOG gene family suggests various roles in establishing plant architecture of Torenia fournieri. *Bmc Plant Biol* 1(18).
32. Phillips HR, *et al.* (2020) Revisiting floral fusion: the evolution and molecular basis of a developmental innovation. J Exp Bot.
33. Ding B, *et al.* (2018) Developmental genetics of corolla tube formation: role of the tasiRNA-ARF pathway. bioRxiv.
34. Wu X, *et al.* (2012) The tobacco BLADE-ON-PETIOLE2 gene mediates differentiation of the corolla abscission zone by controlling longitudinal cell expansion. Plant Physiol 2(159): 835–850.

35. Hay A,Tsiantis M (2010) KNOX genes: versatile regulators of plant development and diversity. Development 19(137): 3153–3165.
36. Jun JH, *et al.* (2010) BLADE-ON-PETIOLE1 coordinates organ determinacy and axial polarity in arabidopsis by directly activating ASYMMETRIC LEAVES2. Plant Cell 1(22): 62–76.
37. Guo M, *et al.* (2008) Direct repression of KNOX loci by the ASYMMETRIC LEAVES1 complex of Arabidopsis. Plant Cell 1(20): 48–58.
38. Khan M, *et al.* (2012) Antagonistic interaction of BLADE-ON-PETIOLE1 and 2 with BREVIPEDICELLUS and PENNYWISE regulates Arabidopsis inflorescence architecture. Plant Physiol 2(158): 946–960.
39. Ma X, *et al.* (2015) A Robust CRISPR/Cas9 System for Convenient, High-Efficiency Multiplex Genome Editing in Monocot and Dicot Plants. Mol Plant 8(8): 1274–1284.
40. Aida R (2012) A protocol for transformation of Torenia. Methods Mol Biol 847): 267–274.
41. Kumar S, *et al.* (2018) MEGA X: Molecular Evolutionary Genetics Analysis across Computing Platforms. Mol Biol Evol 6(35): 1547–1549.
42. Coen ES, *et al.* (1990) floricaula: a homeotic gene required for flower development in antirrhinum majus. Cell 6(63): 1311–1322.
43. Su S, *et al.* (2018) Transcriptome-Wide Analysis Reveals the Origin of Peloria in Chinese Cymbidium (Cymbidium sinense). Plant Cell Physiol 10(59): 2064–2074.
44. Okuda S, *et al.* (2013) Acquisition of LURE-binding activity at the pollen tube tip of Torenia fournieri. Mol Plant 4(6): 1074–1090.

Figures

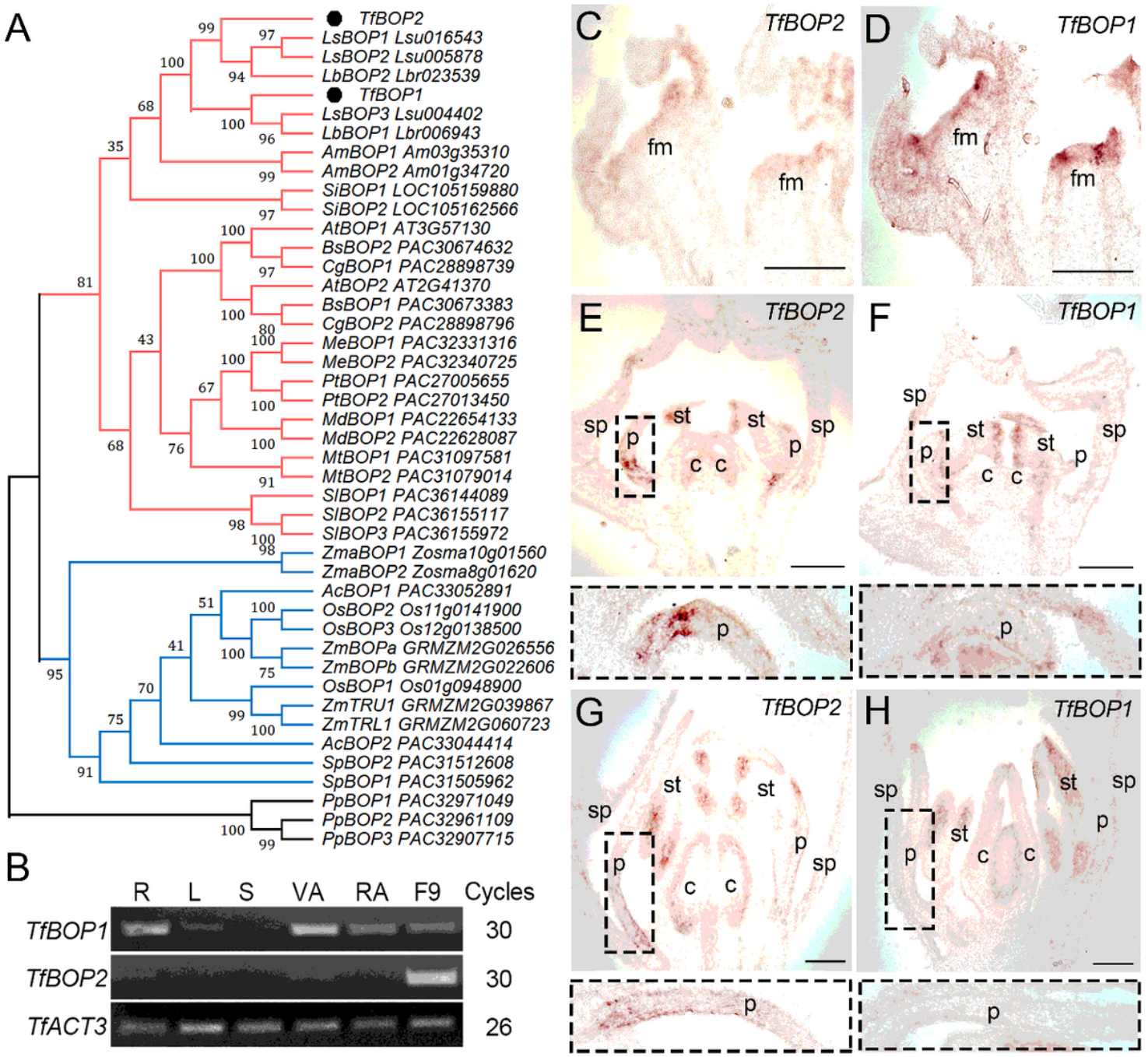

Figure 1

Phylogenetic and expressional analysis of *BOP* genes. (A) Maximum-likelihood tree of *BOP*-like genes from *Physcomitrella patens* (*Pp*), *Spirodela polyrhiza* (*Sp*), *Ananas comosus* (*Ac*), *Zostera marina* (*Zma*), *Oryza sativa* (*Os*), *Zea mays* (*Zm*), *Solanum lycopersicum* (*Sl*), , *Medicago truncutula* (*Mt*), *Malus domestica* (*Md*), *Populus trichocarpa* (*Pt*), *Manihot esculenta* (*Me*), *Arabidopsis thaliana* (*At*), *Boechera stricta* (*Bs*), *Capsella grandiflora* (*Cg*), *Sesamum indicum* (*Si*), *Antirrhinum majus* (*Am*), *Lindernia brevidens* (*Lb*), *Lindernia subracemosa* (*Ls*) and *Torenia fournieri* (*Tf*). Genes from *P. patens* were chosen as outgroups; Branches of monocots and dicots genes were highlighted by blue and red, respectively; 500 times of bootstrap (percentage) is marked at each node and the accession number is included as a suffix of each sequence. (B) Reverse transcription polymerase chain reaction (RT-PCT) analysis of *TfBOP1* and

TfBOP2 in different tissues. Gene names and PCR cycles are shown on the left and right sides of each panel, respectively. *β-actin* (*TfACT3*) was used as an internal control. R, root; L, leaf; S, stem; VA, vegetative apexes; RA, reproductive apexes; F9, stage 9 flower bud. (C-H) RNA *in situ* hybridization of *TfBOP1* and *TfBOP2* in stage 0-1 (C-D), stage 6 (E-F) and stage 8 (G-H) flower buds of wild-type using antisense probes. fm, floral meristem; sp, sepal; p, petal; st, stamen; c, carpel; pl, petal lobe. Scale bars: 100 μm.

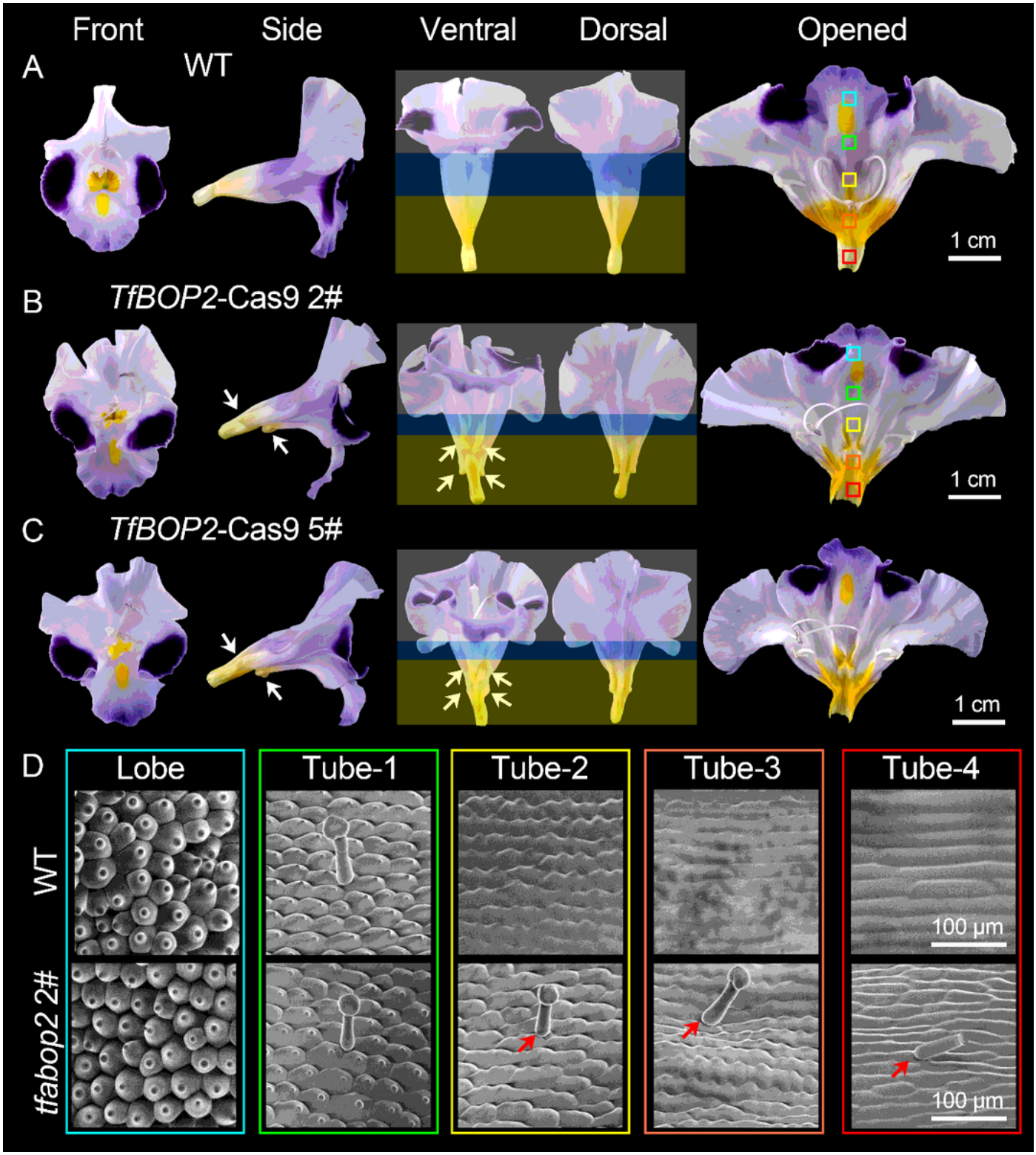

Figure 2

Floral morphologies of wild-type (WT) and TfBOP2-Cas9 mutants. (A-C) Front, side, ventral, dorsal and opened views of WT (A) and two independent *TfBOP2*-Cas9 lines: 2# (B) and 5# (C); Yellow, blue and white blocks indicate the proximal tube, distal tube and lobe regions, respectively; White arrows indicate ectopic tissues in the corollas of *TfBOP2*-Cas9 lines. (D) Corolla epidermal cell morphologies of WT (upper panel) and TfBOP2-Cas9 mutant (lower panel); Whole corollas are divided into five regions along

the proximodistal axis (Lobe, Tube 1/2/3/4) marked by different colors; Red arrows indicate ectopic trichomes on the corollas of *TfBOP2*-Cas9 plants.

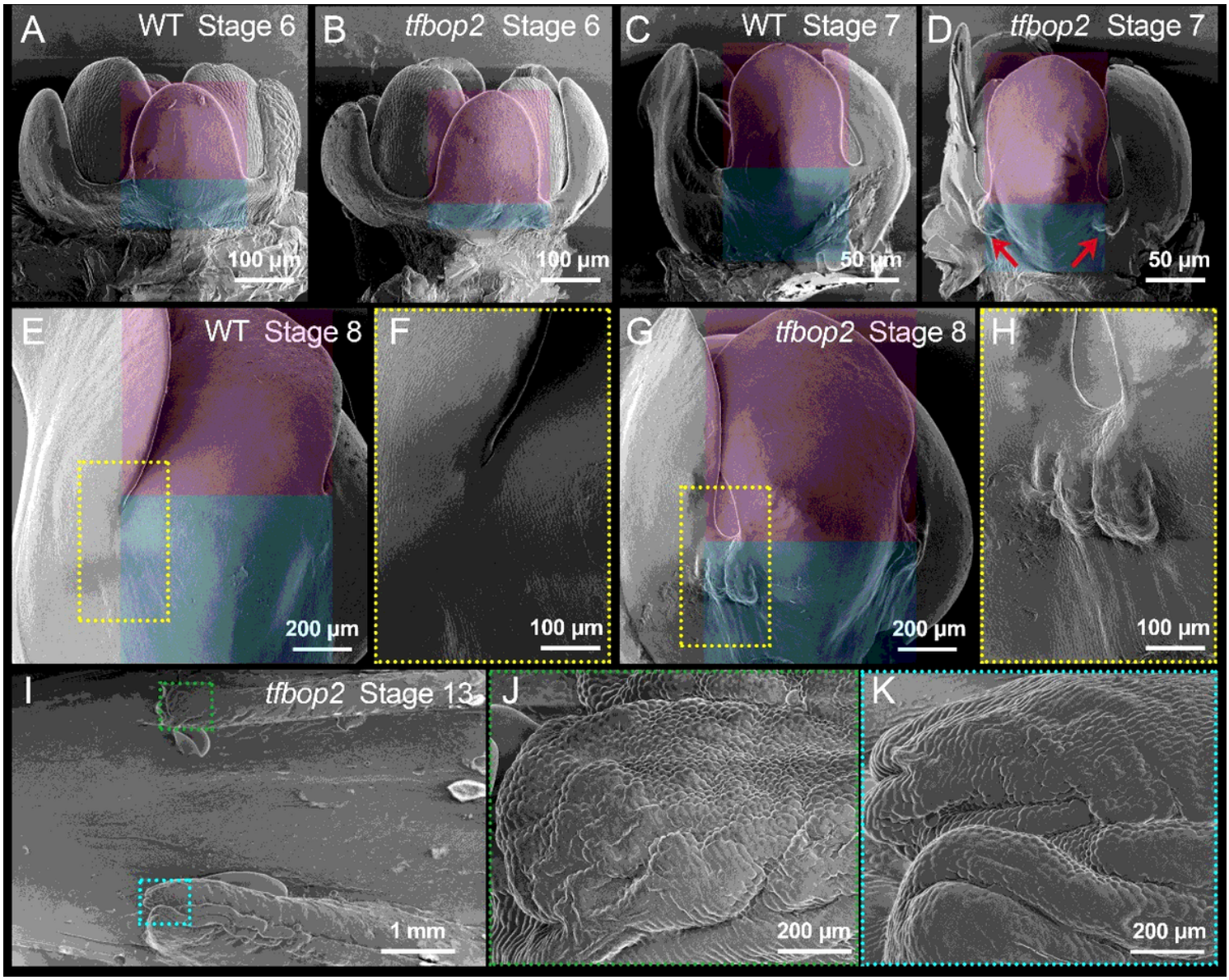

Figure 3

Floral organogenesis of wild-type (WT) and *TfBOP2*-Cas9 plants observed by a scanning electron microscopy. (A-B) Stage 6 flowers of WT and *tfbop2*. (C-D) Stage 7 flowers of WT and *tfbop2*. (E-H) Stage 8 flowers of WT and *tfbop2*. (I) A stage 13 flower of *tfbop2*; (J-K) A zoomed-in view of ectopic tissues in the fusion margins of *tfbop2*. Blue and red blocks indicate the tube and lobe regions, respectively; Red arrows indicate ectopic tissues in the fusion margins of *tfbop2*.

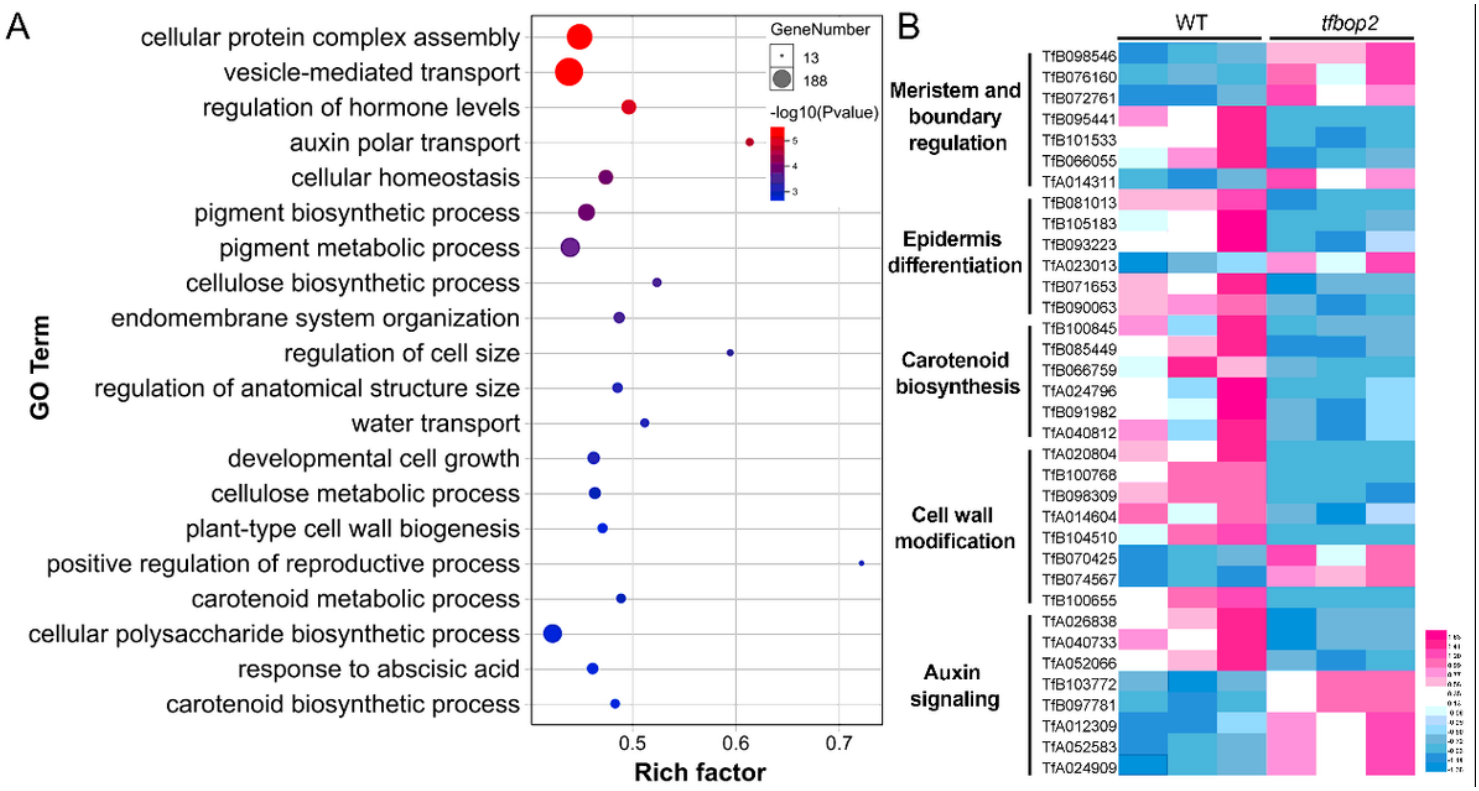

Figure 4

Downstream pathways and candidates of TfBOP2. (A) Differentially enriched Gene Ontology (GO) terms between the corollas of wild-type (WT) and *TfBOP2*-Cas9 2# (*tfbop2*). (B) Heat map of candidate downstream genes from three biological replicates of transcriptomic data.

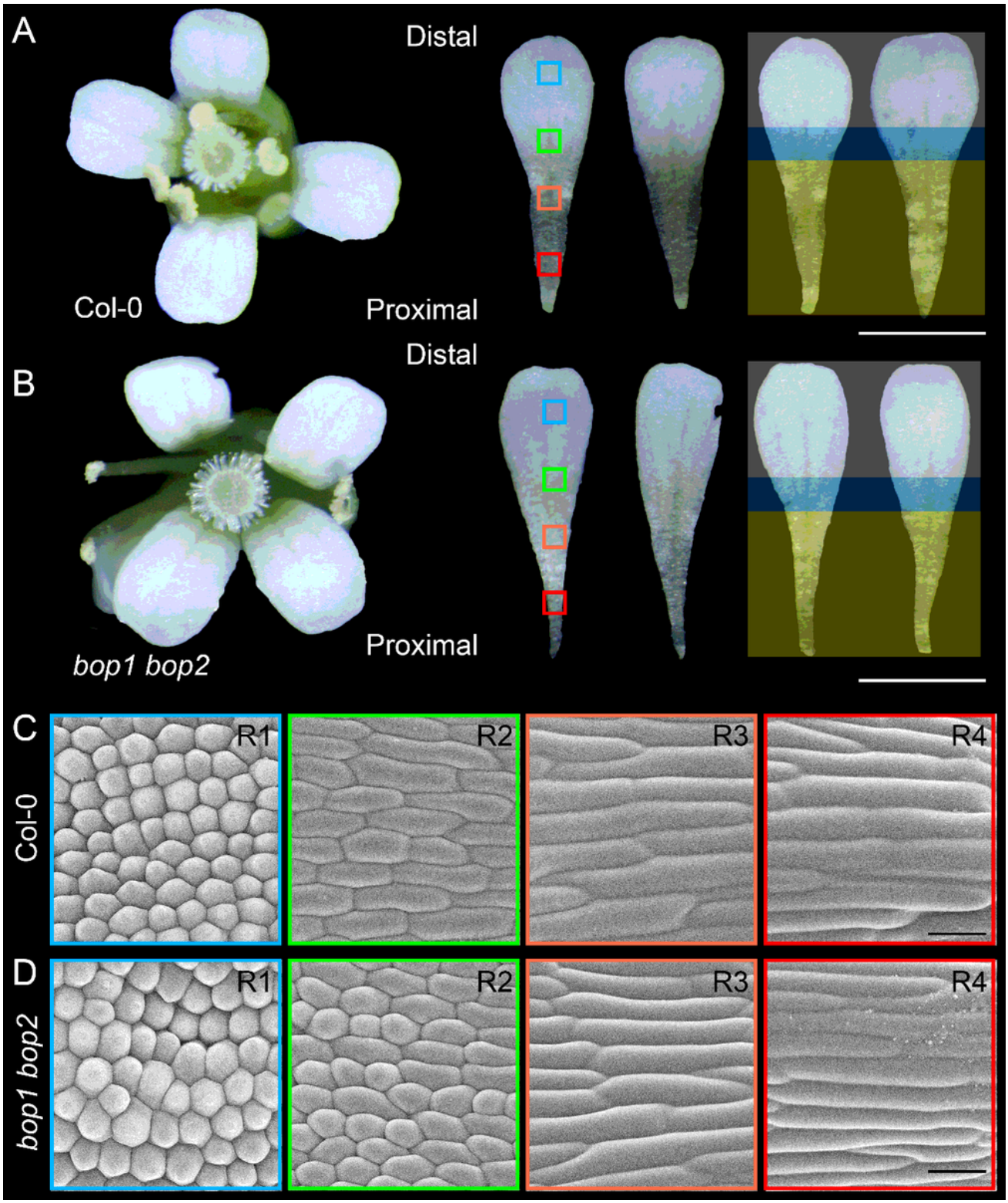

Figure 5

Floral morphologies of wild-type (Col-0) and *bop1 bop2* mutant of *Arabidopsis thaliana*. (A-B) An intact flower and dissected petals of WT (A) and *bop1 bop2* mutant (B); Yellow, blue and white blocks indicate the proximal claw, intermediate and distal blade regions, respectively; Scale bars: 1 mm. (C-D) Corolla epidermal cell morphologies of WT (C) and *bop1 bop2* mutant (D); Whole petal are divided into four regions along the proximodistal axis (R1/2/3/4) marked by different colors; Scale bars: 25 μm.

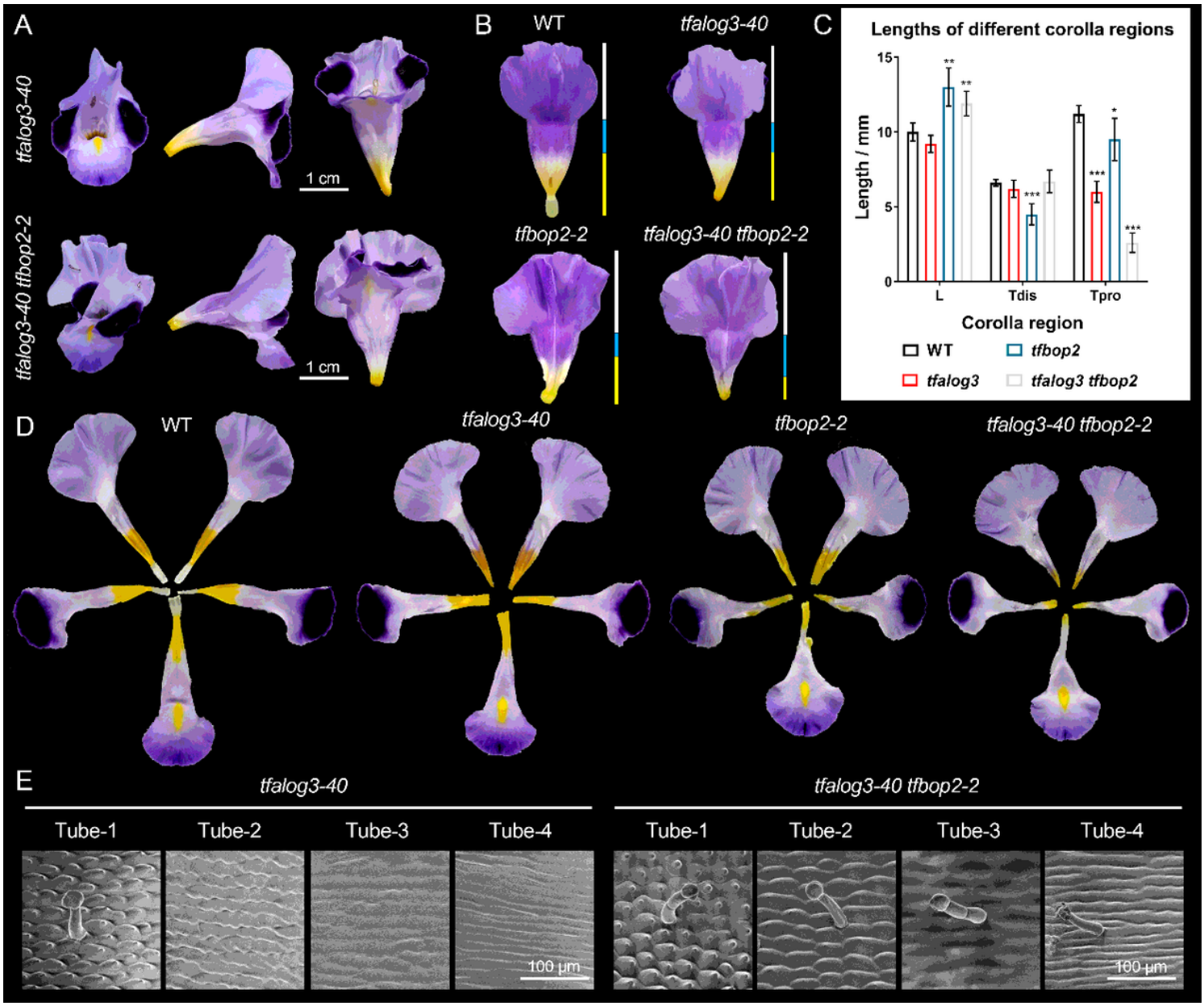

Figure 6

Genetic and physical interaction between TfBOP2 and TfALOG3. (A) Front, side and ventral views of *TfALOG3*-Cas9 40# (*tfalog3-40*) and *TfBOP2*-Cas9 2# *TfALOG3*-Cas9 40# (*tfalog3-40 tfbop2-2*) mutants. (B) Doral views of corollas of different genotypes; Yellow, blue and white bars represent the lengths of proximal tube, distal tube and lobe regions, respectively;. (C) Lengths of different corolla regions (L: lobe; Tdis: distal tube region; Tpro: proximal tube region) of different genotypes; * indicates $p<0.05$; ** indicates $p<0.01$; *** indicates $p<0.001$. (D) Five petals dissected from a typical flower of different genotypes. (E) Corolla epidermal cell morphologies of *tfalog3-40* and *tfalog3-40 tfbop2-2* mutants; T1-T4 represent four regions from distal to proximal regions of corolla tubes.

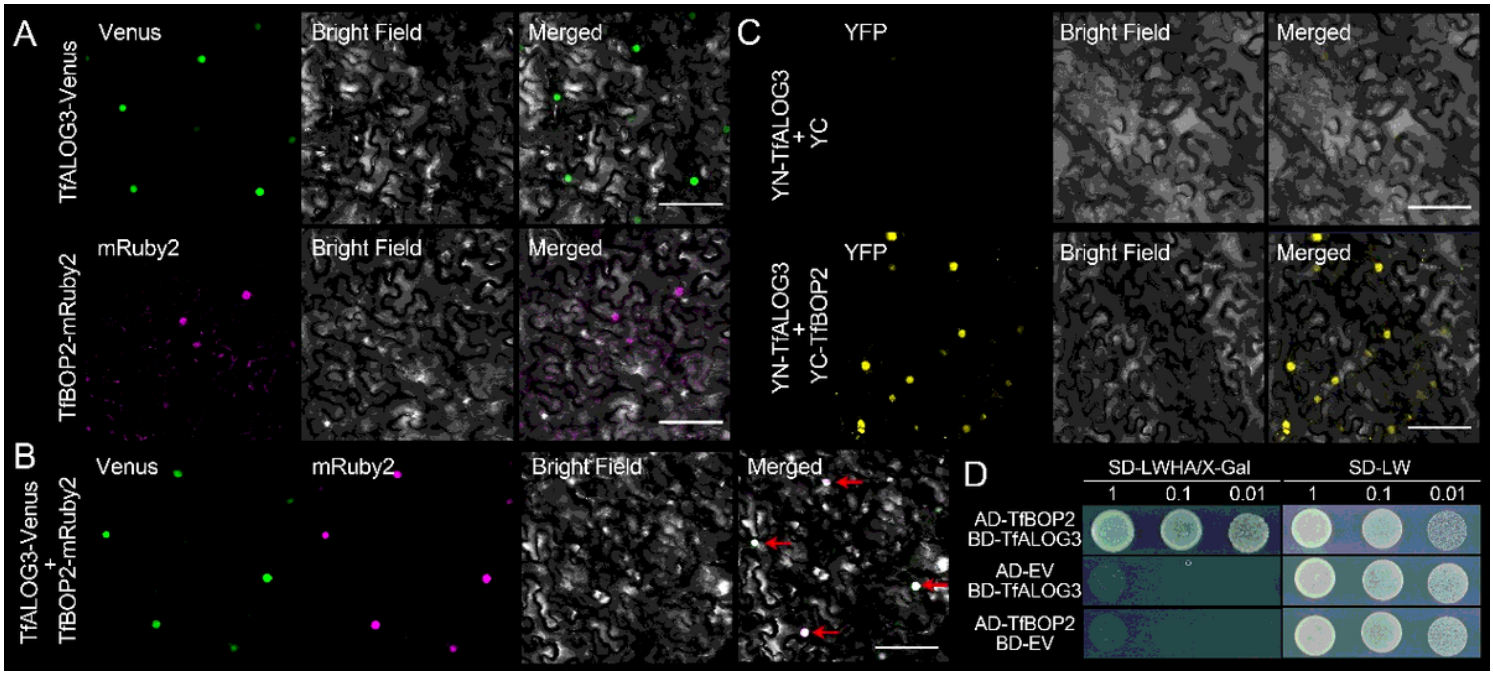

Figure 7

Physical interaction between TfBOP2 and TfALOG3. (A) Subcellular localization of TfALOG3-Venus and TfBOP2-mRuby2 fused proteins in tobacco leaves. Scale bars: 100 μm. (B) Subcellular colocalization of transiently expressed TfALOG3-Venus with TfBOP2-mRuby2 fusion proteins in tobacco leaves. Scale bars: 100 μm. (C) Bimolecular fluorescence complementation (BiFC) assays in tobacco leaves showing TfBOP2 interacts with TfALOG3 in the nucleus. Scale bars: 100 μm. (D) Yeast two-hybrid assays showing that TfBOP2 interacts with TfALOG3. AD and BD represent pGADT7 and pGBKT7 vector, respectively; SD-LWHA/X-Gal and SD-LW indicate selective (SD medium minus Trp, Leu, His, Ade and supplemented with X-α-Gal) and nonselective (SD minus Trp and Leu) media.

Supplementary Files

This is a list of supplementary files associated with this preprint. Click to download.

- Tab.S1DEG.csv
- Tab.S2GOBP.xls
- Tab.S3Downstream.xls
- Tab.S4Primers02.xlsx
- BOP2SI02.docx